

Flow over sinusoidal, porous sandbed

Tim-Frederik Dauck

October 22, 2014

Contents

1	1 Introduction	1
2	2 Potential flow past a rigid, sinusoidal bed	2
3	3 Pressure induced Darcy flow	4
4	4 Physically interesting quantities	5
5	5 Streamline coordinates	7
6	6 Stokes Flow	8
7	A Variables	10

1 Introduction

Due to water flow over the oceanic sediment the porous seabed is often rippled. These obstructions interact with the flow causing pressure gradients to build up, which drive flow through the sediment itself. Similar to surface wave induced flow within the sediment [Shum, 1992, 1993], this is yet another mechanism which facilitates exchange of minerals or Oxygen or there like with the water above[Rutherford and Boyle, 1995, Huettel et al., 1996, Evrard et al., 2012]. The flow considered is very similar to wind interacting with dunes, which also drives a flow through the porous sand and for example transports humidity into the sand [Louge et al., 2010]

So far this flow has been studied experimentally Savant et al. [1987], Thibodeaux and Boyle [1987], Louge et al. [2010], Musa et al. [2013] and numerically Meysman et al. [2007] there have been no attempts at finding an analytical solution for this flow.

There are several decisions to be made for setting up a model. One is whether to include turbulence or not and if Reynolds numbers are assumed low or high. The situation on the continental shelf differs in this respect from the situation of oceanic currents. Kuzan et al. [1989] found that for a solid wavy interface with the flow parameters as we would expect them on the continental shelf, there is most likely flow separation and hence turbulence. Another is the form of the boundary condition at the permeable interface. The boundary may be realised by the following approaches:

- Slip condition as described by Beavers and Joseph [1967] with Darcy's law within the porous medium

- 32 • A Brinkman layer within the porous medium by using including the Brinkman term to
33 the Darcy equation, together with continuity of the flow variables
- 34 • A solid interface with Darcy flow in the porous medium driven by the pressure at the
35 boundary.
- 36 • A solid boundary as above, but including roughness (only applicable for turbulent flows)

37 Here we assumed a flow at infinite Reynolds numbers, i.e. Euler flow or potential flow. In
38 this case we can only impose a kinetic boundary condition which assumes a rigid wall. The
39 plan is to perturb the found solution, assuming high but finite Reynolds numbers and small
40 slopes, and impose the Beavers-Joseph boundary condition on this perturbed flow. This would
41 be a solution of potential flow with a friction boundary layer. This still might severely limit
42 the applicability of the model as turbulence was ignored. The set-up is depicted in [Figure 1](#)

43 The plan of work progress is:

- 44 • solve inviscid irrotational flow in the fluid assuming a rigid boundary
- 45 • obtain the streamline-coordinates (potential function and stream function)
- 46 • add a boundary layer, i.e. perturb and assume:
 - 47 – standard boundary layer character (gradient mainly perpendicular)
 - 48 – only a small perturbation to the inviscid solution
- 49 • obtain a formula for the perturbed streamfunction and boundary pressure
- 50 • match series coefficients by using full Beavers-Joseph condition
- 51 • use perturbed pressure at boundary to obtain corrected Darcy Flow

52 As an alternative approximation the situation is analysed employing the slow viscous as-
53 sumption of Stokes flow.

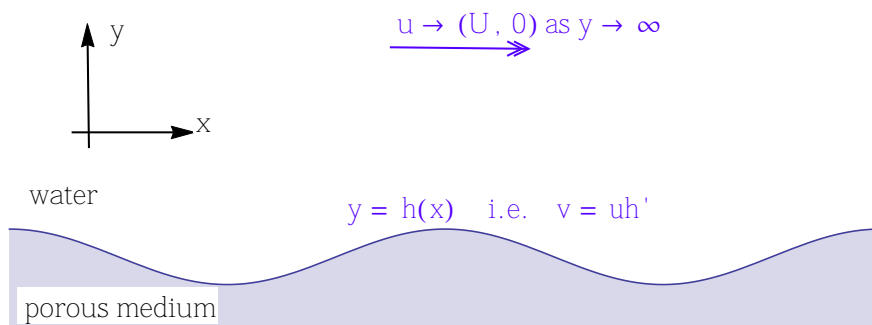


Figure 1: Problem analysed

54 2 Potential flow past a rigid, sinusoidal bed

As a first approximation, the flow is assumed to be inviscid. Having no initial vorticity we get potential flow, i.e. we can write $\mathbf{u} = \nabla\phi$ for some function $\phi(x, y)$. Incompressibility of the flow gives Laplace's equation (1a). The boundary conditions are the far field condition

of exterior flow $\mathbf{u} = (U, 0)$ (1b) and to leading order a stationary boundary at the sinusoidal surface $y = h(x) = \epsilon/k \cos(kx)$ (1c).

$$\begin{aligned} \text{Velocity Potential:} & \quad \mathbf{u} = \nabla\phi, & (1a) \\ \text{Continuity Equation:} & \quad \nabla^2\phi = 0, & (1b) \\ \text{Far Field Condition:} & \quad \phi \rightarrow Ux \quad \text{as } y \rightarrow \infty, & (1c) \\ \text{Stationary Boundary:} & \quad \phi_y = h'(x)\phi_x \quad \text{on } y = h(x) & (1d) \end{aligned}$$

First we non-dimensionalise the equations by writing $x^* = kx$, $y^* = ky$, $\phi^* = kU^{-1}\phi$ and $h^* = k\epsilon^{-1}h = \cos(x^*)$. This gives a new, easier system of equations (2) (the asterisks denote dimensionless quantities)

$$\nabla^{*2}\phi^* = 0, \quad (2a)$$

$$\phi^* \rightarrow x^* \quad \text{as } y^* \rightarrow \infty, \quad (2b)$$

$$\phi_{y^*}^* = \epsilon h'^* \phi_{x^*}^* \quad \text{on } y^* = \epsilon h^*, \quad (2c)$$

55 From now on the asterisks are left out for better readability. An asymptotic solution can
56 be obtained by expanding ϕ (3a) in the slope ϵ and by moving the boundary condition (3b) to
57 $y = 0$ using a Taylor series. These then give an iterative procedure to calculate a series for the
58 potential (4) and (5).

$$\phi = \phi^{(0)} + \epsilon\phi^{(1)} + \epsilon^2\phi^{(2)} + \dots, \quad (3a)$$

$$\phi_y + \epsilon h\phi_{yy} + \frac{1}{2}\epsilon^2 h^2\phi_{yyy} + \dots = \epsilon h'\phi_x + \epsilon^2 h'h\phi_{xy} + \dots \quad \text{on } y = 0 \quad (3b)$$

59 Substituting (3a) into (3b) allows to look at the boundary condition to varying orders in ϵ .

$$\mathcal{O}(1): \quad \phi_y^{(0)} = 0, \quad (4a)$$

$$\mathcal{O}(\epsilon): \quad \phi_y^{(1)} = -h\phi_{yy}^{(0)} + h'\phi_x^{(0)}, \quad (4b)$$

$$\mathcal{O}(\epsilon^2): \quad \phi_y^{(2)} = -h\phi_{yy}^{(1)} - \frac{1}{2}h^2\phi_{yyy}^{(0)} + h'\phi_x^{(1)} + h'h\phi_{xy}^{(0)}, \quad (4c)$$

⋮

$$\mathcal{O}(\epsilon^n): \quad \phi_y^{(n)} = \sum_{i=0}^{n-1} \frac{h^i}{i!} \left(h' \frac{\partial^{i+1}}{\partial y^i \partial x} - \frac{h}{i+1} \frac{\partial^{i+2}}{\partial y^{i+2}} \right) \phi^{(n-1-i)} \quad (4d)$$

60 The solution for the velocity potential can be easily seen as the imaginary part of a complex,
61 analytical function $f(z)$ (6a). From the analysis of complex analytical functions we know that
62 both the real and imaginary part satisfy Laplace's equation. Via the Cauchy-Riemann equations
63 we see that the real part gives the non-dimensional streamfunction $\psi(x, y)$ (6c).

64 The first few explicit calculations (5) of the series in ϕ illustrate the procedure to obtain all
65 terms.

$$\phi^{(0)} = x, \quad (5a)$$

$$\phi_y^{(1)}|_{y=0} = -\sin(x) \quad \Rightarrow \quad \phi^{(1)} = \sin(x)e^{-y} \quad (5b)$$

$$\phi_y^{(2)}|_{y=0} = -\cos(x)\sin(x) - \sin\cos(x) = -\sin(2x), \quad \Rightarrow \quad \phi^{(2)} = \frac{1}{2}\sin(2x)e^{-2y} \quad (5c)$$

⋮

⋮

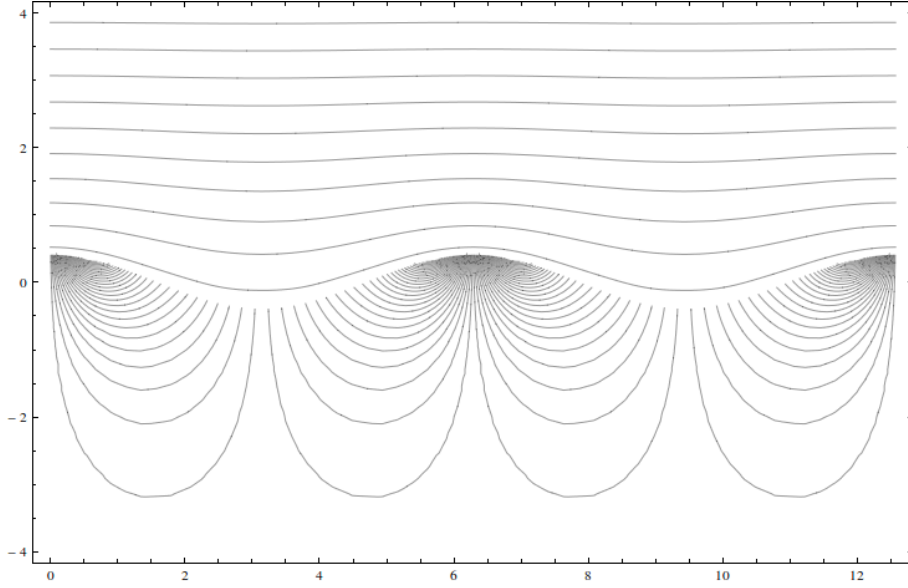


Figure 2: Streamlines of the solution in the water and in the porous sediment

$$f(z) = iz + \epsilon e^{iz} + \frac{\epsilon^2}{2} e^{2iz} + \frac{\epsilon^3}{8} (3e^{3iz} + e^{iz}) + \dots, \quad (6a)$$

$$\phi(x, y) = \text{Im } f(x + iy) = x + \epsilon \sin(x)e^y + \dots, \quad (6b)$$

$$\psi(x, y) = -\text{Re } f(x + iy) = y - \epsilon \cos(x)e^y + \dots \quad (6c)$$

66 Now Bernoulli's equation is applied to obtain the pressure at the boundary. Note that the
 67 pressure is non-dimensionalised by the group ρU^2 . As expected this scaling shows that the
 68 hydrostatic pressure is a effect of order $\mathcal{O}(\epsilon)$. We get a pressure in phase with the ripples,
 69 which is not supported by experiments, but is due to the simplification of ignoring the friction
 70 boundary layer and turbulence.

$$\text{const} = p + \frac{1}{2} |\nabla \phi|^2 + \frac{gy}{U^2 k} \quad (7a)$$

$$p_{bdy}(x) = \text{const} - \frac{g\epsilon}{U^2 k} \cos(x) - \frac{1}{2} (1 + 2\epsilon \cos(x) + \dots) \quad (7b)$$

$$= - \left(1 + \frac{g}{U^2 k}\right) \epsilon \cos(x) + \dots, \quad \text{wlog const} = \frac{1}{2}$$

71 **3 Pressure induced Darcy flow**

To find the flow in the sediment we use Darcy's Law in a non-dimensional form, with the pressure from the fluid solution and decay at $y = -\infty$:

$$\mathbf{u}_D = Da Re \nabla p \quad (8a)$$

$$Da = \kappa k^2 \quad (8b)$$

$$Re = \frac{U}{k\nu} \quad (8c)$$

72 We additionally have continuity $\nabla \cdot \mathbf{u}_D = 0$ which gives Laplace's equation $\nabla^2 p = 0$.

73 Again expand as a series in ϵ

$$p = p^{(0)} + \epsilon \cdot p^{(1)} + \epsilon^2 \cdot p^{(2)} + \dots \quad (9)$$

74 and match orders of ϵ

$$p^{(0)} + \epsilon \cdot p^{(1)} + \epsilon^2 \cdot p^{(2)} + \dots = p_{bdy}(x) = - \underbrace{\left(1 + \frac{g}{U^2 k}\right)}_{=\beta} \epsilon \cos(x) + \dots \quad (10)$$

75 Again this can be solved by means of a complex function, giving a potential and stream-
76 function for the flow velocity inside the sediment.

$$f(z) = \underbrace{\mathcal{D}a\mathcal{R}e\beta\epsilon}_{=A} e^{-iz} + \dots \quad (11a)$$

$$\phi(x, y) = \text{Re } f(x + iy) = A \cos(x)e^y + \dots = \mathcal{D}a\mathcal{R}e \cdot p(x, y) \quad (11b)$$

$$\psi(x, y) = \text{Im } f(x + iy) = -A \sin(x)e^y + \dots \quad (11c)$$

77 4 Physically interesting quantities

78 To obtain physical interesting quantities like flow times and fluxes we restrict ourselves to
79 first order in ϵ . Also we assume a sinusoidal solution for the streamfunction with amplitude
80 $A = \mathcal{O}(\epsilon)$ and possible phase shift θ .

$$\text{streamfunction :} \quad \psi = -A \sin(x + \theta)e^y, \quad (12a)$$

$$\text{flow velocity :} \quad \mathbf{u}_D = (-\sin(x + \theta), \cos(x + \theta)) \cdot Ae^y, \quad (12b)$$

$$\text{outwards surface normal :} \quad \mathbf{n} = (\epsilon \sin(x), 1) \quad (12c)$$

81 We will require two scalar path integrals. The first one being an infinitesimal part of the
82 sand-water boundary. The line element ds is approximated to first order in ϵ .

$$\Gamma_{x^*} : \mathbf{x}(\lambda) = (\lambda, \epsilon \cos(\lambda)) \quad \lambda \in [x^*, x^* + \delta x^*], \quad (12da)$$

$$\int_{\Gamma_{x^*}} \cdot ds = \int_{x^*}^{x^* + \delta x^*} \cdot \sqrt{1 + \epsilon^2 \sin^2(\lambda)} d\lambda \approx \int_{x^*}^{x^* + \delta x^*} \cdot d\lambda, \quad (12db)$$

83 The second one being the integral along the individual pathlines, which are equivalent to
84 streamlines and streaklines for a stationary flow like in this case. Hence the path equation
85 is derived from $\psi_0(x^*) = \text{const} = -A \sin(x + \theta)e^y$. The end points x^* and x^{**} come from
86 the intersection of this with $y = \epsilon \cos(x)$ which to leading order gives the equation $\psi_0(x) \approx$
87 $-A \sin(x + \theta)$.

$$\gamma_{x^*} : \mathbf{x}(\lambda) = \left(\lambda, \ln \left(\frac{\psi_0(x^*)}{A} \csc(\lambda + \theta) \right) \right), \quad (12ea)$$

$$\int_{\gamma_{x^*}} \cdot ds = \int_{x^*}^{x^{**}} \cdot \csc^2(\lambda + \theta) d\lambda, \quad (12eb)$$

$$x^{**} = \pi - x^* - 2\theta + 2N\pi \quad N \in \mathbb{Z} \quad (12ec)$$

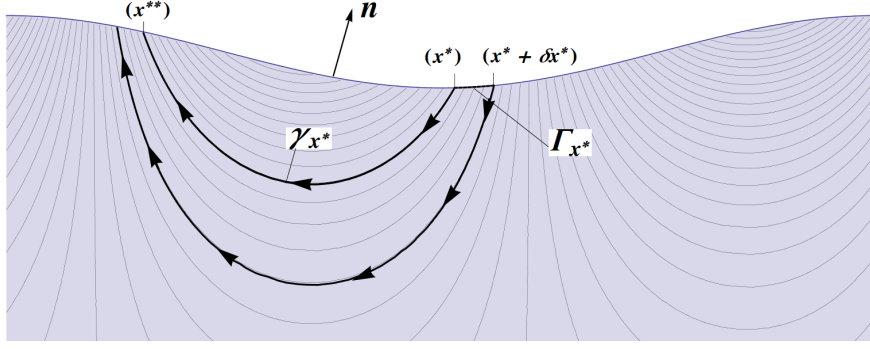


Figure 3: Streamlines of the solution in the water and in the porous sediment

88 Using this we can get some physically interesting quantities, all per unit length in z-direction
 89 and per wave length. First, the flux Φ through an infinitesimal part of the boundary

$$\begin{aligned} \Phi(x^*) &= \int_{\Gamma_{x^*}} \mathbf{u}_D \cdot (-\mathbf{n}) \, ds = \int_{x^*}^{x^* + \delta x^*} (-A \cos(\lambda + \theta) + \mathcal{O}(A\epsilon)) \, d\lambda \\ &= -A \cos(x^*) \delta x^* + \mathcal{O}(A\epsilon + A(\delta x^*)^2) \end{aligned} \quad (6)$$

90 Second, the flow time T for a specific entry point x^* . Using the absolute value we do not
 91 need to fix the value of x^{**} as the periodicity with $2N\pi$ only affects the sign, i.e. set $N = 0$.

$$\begin{aligned} T(x^*) &= \int_{\gamma_{x^*}} |\mathbf{u}_D|^{-1} \, ds \approx \left| \int_{x^*}^{x^{**}} \frac{1}{A} e^{-y} \csc^2(\lambda + \theta) \, d\lambda \right| \\ &\approx \left| \int_{x^*}^{x^{**}} \frac{\sin(\lambda + \theta)}{\psi_0(x^*)} \csc^2(\lambda + \theta) \, d\lambda \right| = \left| \frac{1}{\psi_0(x^*)} \left[\ln \left(\tan \left(\frac{\lambda + \theta}{2} \right) \right) \right]_{x^*}^{x^{**}} \right| \\ &\approx \frac{1}{A} |\csc(x^* + \theta)| \cdot \ln \left(\tan^2 \left(\frac{x^* + \theta}{2} \right) \right) \end{aligned} \quad (7)$$

92 Finally these two combined give the rate of added particles to the main water body due to
 93 washing out within the sand. Where we are given some $\Delta c(T, c_0)$ describing the increase in
 94 concentration of water with a effective concentration c_0 over a flow time of T throughout the
 95 sand. c_0 is the difference of concentrations of the water concentration in the fluid body and
 96 the sand reference concentration. Hence after infinite time spend in the sand a fluid parcel has
 97 $c_0 = 0$.

98 The boundaries of the integral mark the regional change from inflow into the sand to outflow,
 99 which can be seen from the sign change of $\mathbf{u}_D \cdot \mathbf{n} \approx \cos(x + \theta)$.

100 We hence get an expression for the particle increase added to the fluid body from washing
 101 out.

$$\frac{dn_0}{dt} = \int_{\pi/2-\theta}^{3\pi/2-\theta} \Delta c(T(x^*), c_0) \underbrace{(-A \cos(x^*))}_{\Phi(x^*)} \, dx^* \quad (8)$$

102 If we now assume an exponential exchange with a constant concentration of c_s i.e. $\Delta c(T, c_0) =$
 103 $(e^{-\gamma T} - 1) c_0$ we can determine the first order macroscopic exchange rate. To do this note that
 104 for small ϵ we have small A and hence large $T(x^*)$. This means that to leading order $\Delta c \approx 1$
 105 and hence we get the total flux.

$$\frac{dn_0}{dt} \approx \int_{\pi/2-\theta}^{3\pi/2-\theta} (c_s - c_0) (-A \cos(x^*)) \, dx^* = -A \cos(\theta) c_0 \quad (9)$$

106 Note that c_0 and n_0 are closely related as they describe the concentration and the particle
 107 number, respectively, in the fluid body.

Now in the case of purely potential flow we have obtained the results as follows:

$$\theta = 0 \quad (10a)$$

$$A = \mathcal{D}a\mathcal{R}e\beta\epsilon = \kappa k^2 \frac{U}{k\nu} \left(1 + \frac{g}{U^2 k}\right) \epsilon = \frac{\kappa k U \epsilon}{\nu} + \frac{\kappa g \epsilon}{\nu U} = (kU^2 + g) \frac{\kappa \epsilon}{\nu U} \quad (10b)$$

108 This in particular implies that A is equal to the global exchange rate to leading order.

109 For this result to be accurate we need: $\mathcal{R}e \gg 1$, $\mathcal{D}a \ll 1$ and $\epsilon \ll 1$. But also $\mathcal{R}e$ cannot be
 110 too big as otherwise we get recirculation, turbulence or even sand liquefaction. Unfortunately
 111 the pressure is not linear in the sinusoidal disturbance and hence this does not provide a method
 112 for arbitrary disturbances.

113 Hence the final result is in dimensional form:

$$\frac{d n_0}{d t} \approx - (kU^2 + g) \frac{\kappa \epsilon}{\nu U} \cdot c_0 \quad (11)$$

114 5 Streamline coordinates

115 Introduce new coordinates defined by the streamfunction $\psi(x, y)$ and the potential function
 116 $\phi(x, y)$. These present a natural coordinates system for developing a boundary layer see [Ben-](#)
 117 [jamin \[1959\]](#). First the equations are developed. This is merely an algebraically difficult task
 118 and hence only the results are stated in form of the vorticity equation, (12), and in form of the
 119 momentum equation, (13). An expression for the tangential shear stress is also found (15). The
 120 boundary conditions are given by mass conservation in normal direction across the boundary
 121 (14a) and the Beavers-Joseph condition on the tangential shear stress and tangential velocity
 122 (14b).

$$\left(\omega_\psi \frac{\partial}{\partial \phi} - \omega_\phi \frac{\partial}{\partial \psi} \right) (\mathcal{J} \nabla^2 \omega) = \mathcal{R}e^{-1} \mathcal{J} \nabla^4 \omega, \quad (12a)$$

$$u = \sqrt{\mathcal{J}} \omega_\psi, \quad v = -\sqrt{\mathcal{J}} \omega_\phi, \quad (12b)$$

$$\mathcal{J} = \phi_x^2 + \phi_y^2 = \phi_x \psi_y - \phi_y \psi_x = \psi_x^2 + \psi_y^2 \quad (12c)$$

$$\mathcal{J} (\omega_\psi \omega_{\phi\psi} - \omega_\phi \omega_{\psi\psi}) + \frac{1}{2} \mathcal{J}_\phi (\omega_\phi^2 + \omega_\psi^2) = -p_\phi + \mathcal{R}e^{-1} (\mathcal{J} \nabla^2 \omega)_\psi \quad (13a)$$

$$\mathcal{J} (\omega_\phi \omega_{\phi\psi} - \omega_\psi \omega_{\phi\phi}) + \frac{1}{2} \mathcal{J}_\psi (\omega_\phi^2 + \omega_\psi^2) = -p_\psi - \mathcal{R}e^{-1} (\mathcal{J} \nabla^2 \omega)_\phi \quad (13b)$$

$$(13c)$$

$$v|_{\psi=0} = v_D|_{\psi=0} = -\mathcal{R}e^{-1} \mathcal{D}a \sqrt{\mathcal{J}} p_\psi \Big|_{\psi=0}, \quad (14a)$$

$$\tau|_{\psi=0} = \mathcal{R}e \mathcal{D}a^{-1/2} (u - u_D)|_{\psi=0} = \mathcal{R}e \mathcal{D}a^{-1/2} \left(u + \mathcal{R}e^{-1} \mathcal{D}a \sqrt{\mathcal{J}} p_\phi \right) \Big|_{\psi=0} \quad (14b)$$

$$\tau = \mathcal{R}e^{-1} \left((\phi_x^2 - \phi_y^2) (\omega_{\psi\psi} - \omega_{\phi\phi}) + 4\phi_x \phi_y \omega_{\phi\psi} - 2\psi_{xy} \omega_\phi + 2\phi_{xy} \omega_\psi \right) \quad (15a)$$

$$\tau \approx \mathcal{R}e^{-1} (\phi_x^2 - \phi_y^2) \omega_{\psi\psi} \quad (15b)$$

123 Note that in these coordinates the irrotational flow solution is simply $\omega = \psi, p = -J/2$.

124 Now the boundary layer solution is sought as a perturbation, i.e. assume a new streamfunc-
 125 tion $\omega = \psi + \tilde{\omega}$. Now two assumptions are made:

- 126 • the standard boundary layer assumption that gradients normal to the boundary are much
 127 larger than gradients perpendicular to it.

$$\frac{\partial}{\partial \phi} \ll \frac{\partial}{\partial \psi} \quad (16)$$

- 128 • the assumption that the perturbation is small

$$\tilde{\omega} \ll \psi \quad (17)$$

129 The first assumption is well established and standardly used in boundary layer type solution.
 130 The second assumption however imposes a bigger problem: as we approach the boundary the
 131 perturbation grows and eventually can no longer be assumed small, especially as the irrotational
 132 streamfunction goes to 0. Hence this makes it impossible to impose the no slip condition, for
 133 example. However, as shall be seen the Beavers-Joseph condition imposes far less perturbation
 134 from the irrotational solution and hence can be imposed. Another limitation is that only one
 135 boundary condition of the two physically necessary can be imposed in this way.

The full system used for the boundary layer is:

$$\zeta_\phi = \mathcal{R}e^{-1} \zeta_{\psi\psi} \quad (18a)$$

$$\zeta = \mathcal{J} \omega_{\psi\psi} \quad (18b)$$

$$p_\phi = \mathcal{R}e^{-1} \zeta_\psi - (\mathcal{J} \omega_\psi)_\phi \quad (18c)$$

$$\zeta \rightarrow 0 \quad \text{as} \quad \psi \rightarrow \infty \quad (18d)$$

$$\zeta(\phi, \psi) = \zeta(\phi + 2\pi, \psi) \quad (18e)$$

$$\frac{\phi_x^2 - \phi_y^2}{\sqrt{\mathcal{J}}} \omega_{\psi\psi}|_{\psi=0} = \frac{\mathcal{R}e^2}{\mathcal{D}a^{1/2}} \omega_\psi|_{\psi=0} + \mathcal{R}e \mathcal{D}a^{1/2} p_\phi|_{\psi=0} \quad (18f)$$

136 This is a simple diffusion equation in the vorticity ζ and hence can be solved by separation of
 137 variables. Imposing both periodicity (??) and decay (??) we can get the general series solution:

$$\zeta = \sum_{n=1}^{\infty} \left(A_n \cos \left(n\phi - \sqrt{n\mathcal{R}e/2} \psi \right) + B_n \sin \left(n\phi - \sqrt{n\mathcal{R}e/2} \psi \right) \right) e^{-\sqrt{n\mathcal{R}e/2} \psi} = \quad (19)$$

139 Notes for further progress:

- 140 • integrate equation to get p as series (IbPs)
- 141 • integrate ζ equation once to replace ω_ψ as series in BC (show principle)
- 142 • plug in series and equate terms (first order only)
- 143 • get solution for p
- 144 • integrate ζ twice to get formula for ω

145 6 Stokes Flow

146 For Stokes flow we can make use of the similarity of the Darcy-Brinkmann-Forcheimer equation
147 and the Navier-Stokes equation, as in this case in both regions the Reynolds number is small.
148 Using a similar formulation as in we find following system:

$$\varepsilon \frac{\partial \mathbf{u}}{\partial t} + \varepsilon^2 \mathbf{u} \cdot \nabla \mathbf{u} = -\nabla p + \tilde{\mu} \nabla^2 \mathbf{u} - B \frac{\mu}{k} \mathbf{u} \quad (20a)$$

$$\nabla \cdot \mathbf{u} = 0 \quad (20b)$$

149 Employing a stream function ψ , non-dimensionalising and ignoring inertial terms, i.e. as-
150 suming stokes flow, we get a simple equation incorporating a discontinuous function $\alpha(x, y)$:

$$151 \quad \nabla^4 \psi = \alpha \nabla^2 \psi \quad (21)$$

152 Notes for further progress:

- 153 • no-slip BC at given depth within sand
- 154 • prescribe velocity at some height above sand
- 155 • periodicity BCs at vertical boundaries
- 156 • solve in rectangular domain
- 157 • note: α is non zero constant in porous region and zero in the fluid

158 A Variables

159

Basic Flow Variables		
Variable	Dimensionalisation	Description
\mathbf{u}	U	velocity of the fluid
ϕ	U/k	velocity potential, $\mathbf{u} = \nabla\phi$
ψ	U/k	streamfunction, $\mathbf{u} = (\psi_y, -\psi_x)$
p	ρU^2	pressure

160

Physical Parameters	
Variable	Description
ϵ	waveslope
k	wavenumber
U	exterior velocity
ρ	density
μ	kinematic viscosity
ν	dynamic viscosity
g	gravity
κ	permeability of the sediment
γ	exchange coefficient
c_0	concentration difference between the sand and the fluid

161

Non-dimensional Quantities		
Variable	Formula	Description
Re	$= U/k\nu$	Reynolds number
Da	$= \kappa k^2$	Darcy number
β	$= (1 + \frac{g}{U^2 k})$	
A	$= Da Re \beta \epsilon$	

162

Path Integration Quantities		
Variable	Dimensionalisation	Description
Γ	U/k	infinitesimal path along sediment boundary
γ	U/k	flow path through sediment
\mathbf{n}	$1/k$	normal to the sediment
ds	$1/k$	infinitesimal arclength element
$\lambda, d\lambda$	$1/k$	alternative parametrisation (in x-direction)

163

Variables related to Boundary Layer Approach		
Variable	Dimensionalisation	Description
ω	U/k	streamfunction of viscos corrected flow
$\tilde{\omega}$	U/k	perturbation to inviscid streamfunction
\mathcal{J}	U^2	jacobian
τ	ρU^2	stress
ζ	Uk	vorticity

164

Variables related to Stokes Flow Approach	
Variable	Description
ϵ	porosity
$\tilde{\mu}$	effective viscosity
B	binary parameter

165

References

Transitional Flow : Darcy-Brinkman Navier-Stokes, 2008.

G. S. Beavers and D. D. Joseph. Boundary conditions at a naturally permeable wall. *Journal of Fluid Mechanics*, 30(01):197–207, Mar. 1967. ISSN 0022-1120. doi: 10.1017/S0022112067001375. URL http://www.journals.cambridge.org/abstract_S0022112067001375.

T. Benjamin. Shearing flow over a wavy boundary. *Journal of Fluid Mechanics*, 6:161–205, 1959. URL http://journals.cambridge.org/abstract_S0022112059000568.

V. Evrard, R. N. Glud, and P. L. M. Cook. The kinetics of denitrification in permeable sediments. *Biogeochemistry*, 113(1-3):563–572, Sept. 2012. ISSN 0168-2563. doi: 10.1007/s10533-012-9789-x. URL <http://link.springer.com/10.1007/s10533-012-9789-x>.

M. Huettel, W. Ziebis, and S. Forster. Flow-induced uptake of particulate matter in permeable sediments. *Limnology and Oceanography*, 41(2):309–322, 1996. URL <ftp://ftp.soest.hawaii.edu/glazer/ChenReferences/Papers1/Huettel1996Flowinduceduptakeofparticulateorganicmatter.pdf>.

J. Kuzan, T. Hanratty, and R. Adrian. Turbulent flows with incipient separation over solid waves. *Experiments in fluids*, 7:88–98, 1989. URL <http://link.springer.com/article/10.1007/BF00207300>.

M. Louge, A. Valance, H. Mint Babah, J.-C. Moreau-Trouvé, and A. Ould el Moutar. Seepage-induced penetration of water vapor and dust beneath ripples and dunes. *Journal of Geophysical Research*, 115(F2):F02002, Apr. 2010. ISSN 0148-0227. doi: 10.1029/2009JF001385. URL <http://doi.wiley.com/10.1029/2009JF001385><http://onlinelibrary.wiley.com/doi/10.1029/2009JF001385/full>.

F. Meysman, O. Galaktionov, P. Cook, F. Janssen, M. Huettel, and J. Middelburg. Quantifying biologically and physically induced flow and tracer dynamics in permeable sediments. *Biogeosciences*, 4:627–646, 2007. URL <http://www.biogeosciences.net/4/627/2007/bg-4-627-2007.html>.

R. Musa, S. Takarrouht, M. Louge, J. Xu, and M. Berberich. Pore pressure in a wind-swept rippled bed. *Journal of Geophysical Research*, 2013. doi: 10.1016/S1571-9197(05)80035-7. URL http://grainflowresearch.mae.cornell.edu/geophysics/dunes/papers/WindTunnelSept13_2013_2Col.pdf.

J. Rutherford and J. Boyle. Modeling benthic oxygen uptake by pumping. *Journal of Environmental Engineering*, 121(1):84–95, 1995. URL [http://ascelibrary.org/doi/abs/10.1061/\(ASCE\)0733-9372\(1995\)121:1\(84\)](http://ascelibrary.org/doi/abs/10.1061/(ASCE)0733-9372(1995)121:1(84)).

S. Savant, D. Reible, and L. Thibodeaux. Convective transport within stable river sediments. *Water Resources ...*, 23(9):1763–1768, 1987. URL <http://onlinelibrary.wiley.com/doi/10.1029/WR023i009p01763/full>.

- 203 K. Shum. Waveinduced advective transport below a rippled watersediment interface. *Journal of*
204 *Geophysical Research: Oceans*, 97(C1):789–808, 1992. URL [http://onlinelibrary.wiley.](http://onlinelibrary.wiley.com/doi/10.1029/91JC02101/full)
205 [com/doi/10.1029/91JC02101/full](http://onlinelibrary.wiley.com/doi/10.1029/91JC02101/full).
- 206 K. Shum. The effects of waveinduced pore water circulation on the transport of reactive solutes
207 below a rippled sediment bed. *Journal of Geophysical Research: Oceans*, 98(C6):10,289–
208 10,301, 1993. URL <http://onlinelibrary.wiley.com/doi/10.1029/93JC00787/full>.
- 209 L. Thibodeaux and J. Boyle. Bedform-generated convective transport in bottom sediment.
210 *Nature*, 325:341–343, 1987. URL [http://www.nature.com/nature/journal/v325/n6102/](http://www.nature.com/nature/journal/v325/n6102/abs/325341a0.html)
211 [abs/325341a0.html](http://www.nature.com/nature/journal/v325/n6102/abs/325341a0.html).